

## FE SIMULATION OF CONTROL SURFACES WITH SMA ACTUATORS FOR SMALL SIZE AIRCRAFTS

V. L. Sateesh, Jaysankar, Senthil Kumar P, Gangadhar Raju S, Sathisha and G. N. Dayananda  
Centre for Societal Missions and Special Technologies, National Aerospace Laboratories, Bangalore, India.  
Email: sateesh@nal.res.in

**Abstract:** In this study an attempt has been made to simulate the control surfaces, which has been equipped with SMA based actuating mechanism for deploying the trim tab, for a small scale aircraft. The existing elevator has been modified to incorporate the shape memory alloy (SMA) mechanism. Analysis of modified elevator with trim tab has been carried out using finite element method. Experimental investigation has also been carried out to validate the theoretical results by mounting the strain gauges in the elevator. The strains obtained from the theoretical study correlate reasonably well with the experimental data. The results of the study clearly show that the stress and strain field of elevator due to the SMA actuation is within the permissible limits.

### 1. INTRODUCTION

Smart materials such as shape memory alloys (SMA) and piezo electric ceramics are promising materials as actuators and sensors [1]. During the recent years there is extensive research being carried out to use these materials for shape control [2-3], vibration and noise control [4-6], and actuating the aerodynamic surfaces [7]. Recently authors [Ref. 8] deployed an additional aerodynamic surface called mousche using the shape memory alloys.

In this study, finite element simulations have been carried out to estimate the forces on the elevator due to the shape memory alloy actuation and aerodynamic loading on the trim tab. The trim tab is a small auxiliary control surface hinged to the elevator of the aircraft. Trim tab is connected to the elevator by a piano hinge and a linking mechanism. Usually, the trim tab is controlled by a servo motor. There are few drawbacks with the servomotors like jamming in the actuated condition. In order to avoid this undesirable condition it is proposed to replace the electrically operated servo motors with shape memory alloy (SMA) mechanisms.

Shape memory alloys are the class of actuators; generate large deformations and forces with the application of temperature and/or pressure. This material undergoes phase transformation from austenite to martensite with the application of mechanical load or change in the ambient temperature. Generally austenite phase is higher temperature phase and the cell structure is in highly symmetric cubic form. The application of mechanical load changes the crystal structure to monoclinic which is a martensitic phase. The change in the phase transformation induces large recoverable strains. By unloading the mechanical loading the martensitic phase reverse transforms to austenitic phase and the residual strains are fully recovered. Therefore this phenomenon is called pseudo elastic shape memory effect or superelastic shape memory effect. Hence this effect is used in the structural damping applications.

On the other hand, the phase transformation can be obtained by lowering the ambient temperature. Reduction in the temperature ends up with forming the martensitic twins in the material. Hence no macroscopic strains are observed in the material. Application of mechanical loading leads to de-twinning the martensite twins and induces residual strains. This residual strain can be recovered by applying the temperature. This effect facilitates that this material can be used as actuator. The schematic representation of the shape memory effect is shown in Fig. 1.

The SMA wires in martensitic phase with de-twinning micro structure are used as actuators replacing servo motors for actuating the trim tab. Application of the temperature changes the micro structure to cubic and hence the SMA wire contracts. To accommodate this SMA system, the existing elevator is modified by constructing additional ribs to take the reactions from the SMA wires. Holes have been drilled to run the SMA wires through the ribs. The details of the modification to the elevator are shown in the Fig. 2 and the details of SMA mechanism are shown in the Fig. 3. One end of the SMA wires is fixed to the rib of the elevator and the other end is connected to the timer belt (Fig. 3). This timer belt is running over the pulleys. These SMA wires act antagonistic to each other.

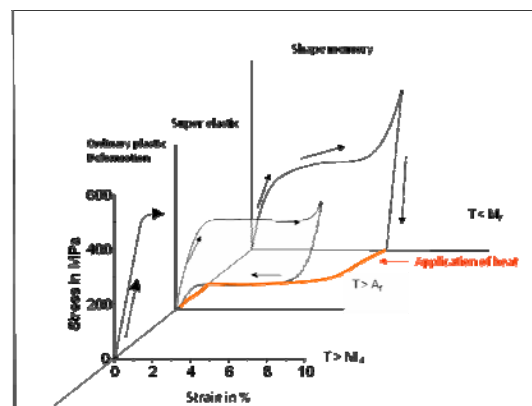


Figure 1 Schematic representation of shape memory effect

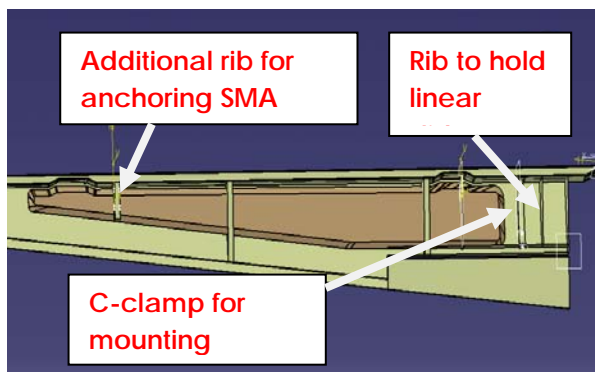


Figure 2. Modified elevator with trim tab

The SMA wires are actuated by Joule heating. The SMA wires contract with the application of heat. This contracted SMA wire pulls the timer belt which is connected to link mechanism. This link mechanism actuates the trim tab. The requirements of actuation are  $31^\circ$  on bottom side and  $21^\circ$  on top side of the trim tab. The trim tab is actuated up by powering the SMA wire near to the trim tab (wire-1) (Fig. 3). The SMA wire-2 (near to the front spar) acts as bias spring for the wire-1. Trim tab can be actuated down by powering wire-2. The actuation of the SMA wires induces axial force on the elevator. In addition aerodynamic loading on the trim tab exerts the force on the SMA mechanism through the connecting links. The resultant forces from aerodynamic loading oppose the SMA force. Hence it is necessary to estimate the forces in the SMA mechanism and the stresses in the modified elevator.

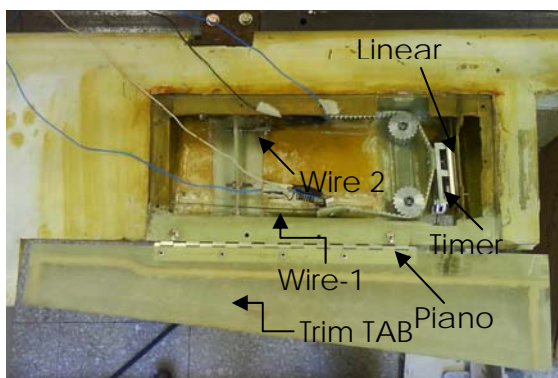


Fig 3. SMA mechanism

Therefore, the objectives of the study are

- i). To analyze the modified elevator to find out the stresses due to actuation of SMA wires and validate with the experimental data.
- ii). To simulate the forces on the SMA actuators due to the aerodynamic loads on the trim tab. The detailed description of the analysis and results are discussed in the following sections.

## 2. ANALYSIS

The analysis of the elevator with the linking mechanism is carried out in two stages. In the first stage, entire SMA mechanism and trim tab links are replaced with only SMA resultant forces i.e. forces due to aerodynamic loads are omitted. The second stage consists of analysis of elevator with trim tab linkage mechanism and pulleys with the timer belt. NASTRAN FE package has been used for the analysis. Initially, solid modeling has been done in the CATIA. All the surfaces in the elevator are discretized with two dimensional CQUAD-4 and CTRIA-3 elements. The details of the finite element mesh are shown in the Fig. 4.

In order to obtain the loads on the elevator due to the SMA actuation, experiments have been carried out on a test jig. While testing, each SMA wire has been actuated at a time and loads were found on both the wires. Load cells were attached to the anchoring end of the SMA wires to measure the forces. Actuation of wire-1 results in a net axial force of 50 kg along with a simultaneous axial contraction of wire. In addition, it exerts 36 kg force in the wire-2. This axial movement is converted to swiveling moment of the trim tab towards the upward direction. Likewise the actuation of wire 2 results in downward movement of the trim tab.

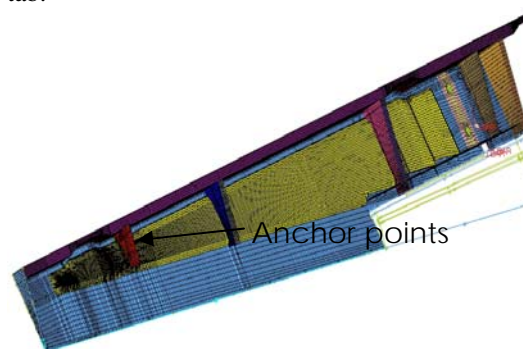


Fig. 4 Discretization of Elevator with CQUAD and CTRIA elements.

### 2.1 Analysis of Elevator without Trim Tab

Analysis of the elevator has been carried out by applying the loads on the anchoring points and pulleys, and the resulting strain field is shown in the Fig. 5. Fixed boundary conditions have been employed at the actual hinge points of the elevator. Experiments have also been carried out to validate the analysis results by strain gauging at two different critical locations that have been identified from the analysis. The details of the strain gauging are shown in the Fig. 6. Each SMA wire is actuated at a time and strain readings are taken at both the locations. Three such readings are taken and the average value is given in table 1. In addition with the experiential data, analysis results are also given in the Table 1. From the Table 1 it is can be seen that the analysis results are satisfactorily capturing the local behavior of the strain field.

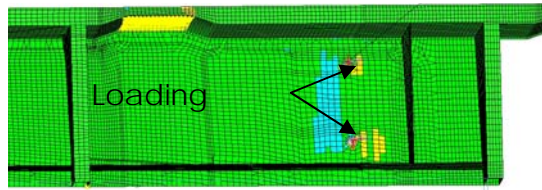


Figure 5 Strain field in the elevator due to SMA actuation.

Table 1 Theoretical and experimental strain field at locations 1 and 2

Strain gauge location	Experimental (micro-strains)		Theoretical (micro-strains)	
	Top	Bottom	Top	Bottom
1	207.5	232	248	245
2	87	101	171	211

Table 2 Theoretical maximum axial stress

Maximum stress MPA	12
--------------------	----

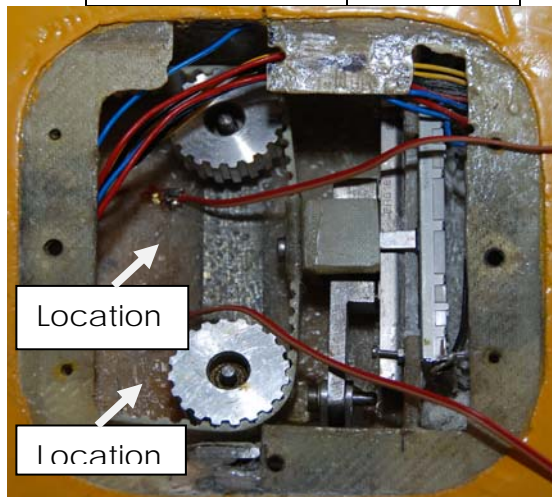


Fig. 6 Strain gauge locations

Further, it can be seen that the predicted strains from the FE analysis are more than that of the experimental results. The difference in the magnitude of the strains may be due to the variation in the loading and the discrepancy in the fabrication, amount of powering given to the SMA wires. From table-2 it can be seen that the stresses are well within the limits.

## 2.2 Analysis of Elevator with Trim Tab

For simulating the exact experimental condition, analysis of the elevator has been carried out with the belt and link mechanism. In the analysis, active SMA wire has been replaced with a force and biasing SMA wire has been replaced with equivalent spring element. Stiffness of the spring element is calculated based on the modulus of the wire in martensitic phase. Finite element model for this simulation is given in the Fig. 7.

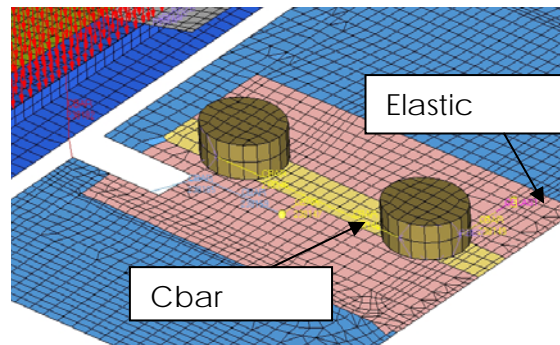


Fig. 7 Details of FE model for timer belt and elastic spring

In the analysis timer belt is replaced with the CBAR elements and pulleys are connect to the elevator by RBAR elements. The rotational degree of freedom has been relaxed for RBAR element to facilitate the rotation of the pulley (Fig. 7). From the wind tunnel data it was found that there is 30 N load acting on the trim tab. In the analysis, it is assumed that this 30 N load is acted uniformly over the entire trim tab. This aerodynamic load is transferred to the linear slide then to the timer belt by links. It is assumed that the linear slider is frictionless and in the analysis, links are directly connected to the timer belt. The links are also modeled with the CBAR elements.

Initially the force due to the SMA actuation has not been included in the analysis, to find the loads that are transferred to the SMA system due to the aerodynamic loads on the trim tab. During this exercise both wires are assumed to be anchored on the other end. The resulting force in the timer belt is found to be 52 N. Finally analysis has been carried out by including the force due to SMA actuation and the aerodynamic loads in the trim tab. The redistributed loads in the timer belt and spring are given in table 3. In the table, the forces in the timer belt and elastic spring are also given when there is no aerodynamic loading. The difference in these two forces gives the redistributed loading due to air load.

Table 3 Forces in various members due to the SMA actuation

Member	Force with aerodynamic loads (N)	Force without aerodynamic load (N)
Spring	309	363
Timer belt	442	428

The forces on the timer belt and spring elements show the modified/reallocated forces due to the loading in the trim tab. So it is necessary during the actuation of the SMA wires to accommodate these additional forces. From the simulations we have been gained the confidence that the strains and stress in the elevator due to the actuation of the SMA are under allowable limits. Hence it can be tested in the wind tunnel safely.

### 3. CONCLUSIONS

Analysis of modified elevator with trim tab for small aircraft has been carried out using finite element method. Experimental investigation has also been carried out to validate the theoretical results by mounting the strain gauges in the elevator. The strains obtained from the theoretical study correlate reasonably well with the experimental data. Further, the results clearly indicate that the strains and stresses due to the SMA actuation forces are within the permissible limits.

### REFERENCES

1. Crawley E F 1994 Intelligent Structures for Aerospace: A Technological Overview and Assessment," AIAA Journal 32 1689-1699.
2. Moallem M "Application of shape memory alloy actuators for flexure control: Theory and experiments" IEEE Transaction of Mechatronics, Vol. 10, No. 5, 2005.
3. B N Agrawal and K E Treanor "Shape control of a beam using piezoelectric actuators" Smart Materials and Structures, Vol. 8, pp. 729-740, 1999.
4. Narayanan, S., and Balamurugan, V., "Finite Element Modelling of Piezolaminated Smart Structures for Active Vibration Control with Distributed Sensors and Actuators" Journal of Sound and Vibration, Vol. 262, pp. 529-562, 2003.
5. Y-R Hu, A Ng "Active robust vibration control of flexible structures," Vol. 288, No. 43-56, 2005.
6. Z-C Qiu, J Han, X-m Zhang, Y Wang and Z Wu "Active vibration control of a flexible beam using a non-collocated acceleration sensor and piezoelectric patch actuator" Journal of Sound and Vibration," Vol. 326, No. 3-5, pp. 438-455, 2009.
7. Song G and Ma N "Robust control of a shape memory alloy wire actuated flap" Smart materials and structures, Vol. 16, pp. N51-N57, 2007.
8. S Jayasankar, P Senthil Kumar, Byji Varughese, B Ramanaiiah, Satisha, H V Ramachandra and G N Dayananda, "Smart Deployment of an Aerodynamic Surface for a Typical Military Aircraft using Shape Memory Elements," Communicated to JIM